Food Chemistry: X 24 (2024) 101839

Contents lists available at ScienceDirect

Food Chemistry: X

journal homepage: www.sciencedirect.com/journal/food-chemistry-x

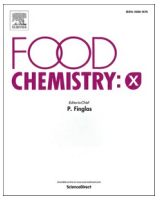

Arginine as a regulator of antioxidant and gel formation in yak Myofibrillar proteins: Efficacy and mechanistic insights

Yuqi Wang [a], Yiwen Mei [a], Rongsheng Du [b], Shulin Zhang [a], Qiuyu Wang [a], Xiaofang Dao [a], Na Li [c], Lina Wang [a], Linlin Wang [a,*], Honghong He [d,*]

[a] College of Food Science and Technology, Southwest Minzu University, Chengdu, Sichuan 610041, PR China
[b] Sichuan Institute of Musk Deer Breeding, Chengdu, Sichuan 610016, PR China
[c] College of Veterinary Medicine, Xinjiang Agricultural University, Urumqi City, Xinjiang 830000, China
[d] College of Animal Science and Veterinary Sciences, Southwest Minzu University, Chengdu, Sichuan 610041, PR China

ARTICLE INFO

Chemical compounds studied in this article:
Arginine (PubChem CID: 6322)
Phosphate (PubChem CID: 1061)
NaCl (PubChem CID: 5234)
DNPH (PubChem CID:3772977)
Trichloroacetic acid (PubChem CID: 6421)
Guanidine hydrochloride (PubChem CID:35742)
Urea (PubChem CID: 1176)
Sodium dodecyl sulfate (PubChem CID:3423265)
Bromophenol blue (PubChem CID: 8272)

Keywords:
Arginine
Meat additives
Antioxidant
Myofibrillar protein
Gelation
Yak meat

ABSTRACT

Arginine (Arg), a safe basic amino acid, modulates interprotein interactions and impacts the processing characteristics of myofibrillar proteins (MP) in meat products, as numerous studies have demonstrated. This study aimed to explore the effects of varying concentrations of Arg (0.025, 0.050, 0.100, 0.200 %) on the physicochemical properties and gel behavior of yak MP. Utilizing yak MP as the substrate, we assessed and analyzed the physicochemical attributes and gel performance of the MP-Arg composite system. The findings revealed that Arg facilitates MP unfolding and internal group exposure, effectively mitigating oxidative tertiary structure alterations. Arg exerts potent antioxidant activity on MP, augmenting their water-holding capacity, which ameliorates gel properties. In this experiment, 0.05 % Arg maximally inhibited oxidative damage to MP, with protection being concentration-dependent. Collectively, these findings suggest that Arg effectively inhibits the oxidative degradation of MP structure and promotes the formation of enhanced gel characteristics.

1. Introduction

The yak "*Bos grunniens*" is an iconic species that lives at high altitudes on the Tibetan Plateau, and is the main species of livestock raised by high-altitude Tibetans living on the Tibetan Plateau and neighboring regions (Gu, 2024). The yak lives at altitudes between 2000 and 5000 m above sea level, and these environments are characterized by low temperatures, low oxygen and intense solar radiation, creating yak specificity and naturalness (Guo et al., 2021). Yak meat is distinguished by its high protein content, ranging from 21.13 % to 23.35 %, and a comparatively lower fat content, varying from 1.60 % to 3.45 %. It encompassing all eight essential amino acids as well as non-essential ones. Additionally, yak meat boasts a significant proportion of polyunsaturated fatty acids, with a relative content between 35 % to 45 %. This nutritional profile is beneficial in the reduction of cardiovascular disease risk (Li, He, et al., 2023). Yak meat has become a natural green meat product that is more in line with human health needs in the new era due to its high nutrition, mineral and protein content and lower fat content.

The postmortem aging of meat is a multifaceted biochemical and metabolic phenomenon, encompassing processes such as apoptosis, protein hydrolysis, and lipid oxidation. These intricate mechanisms are crucial for enhancing meat tenderness, texture, and quality, as reported by (Bu et al., 2023). Empirical data show that prolonged postmortem aging and storage lead to increased cooking loss and decreased water retention. Such alterations can culminate in a diminished quality and

* Corresponding authors.
E-mail addresses: jiayouwl123@163.com (L. Wang), honghong3h@126.com (H. He).

https://doi.org/10.1016/j.fochx.2024.101839
Received 17 July 2024; Received in revised form 12 September 2024; Accepted 15 September 2024
Available online 16 September 2024

nutritional value of yak meat. Specifically, processing of meat products is a key determinant of quality degradation, as detailed in (Grasso et al., 2024). The intrinsic quality traits of meat products, including color, tenderness, and flavor, are paramount determinants of consumer purchasing decisions. Therefore, the enhancement of these quality characteristics is an imperative prerequisite for bolstering the marketability of meat products.

Myofibrillar protein (MP) make up 50–55 % of the total proteins and have thermally induced gelation properties that determine the quality and functionality of the meat (Zhang, Tian, et al., 2022). MP are composed of myosin, actin, troponin, and tropomyoglobin, among others. Myosin is the dominant component in the formation of MP gels. MP are susceptible to oxidation, with myosin being the most sensitive of these proteins (Yu et al., 2024). MP oxidation is typically the result of a covalent modification of proteins induced by reactive oxygen species and secondary by-products of oxidative stress. The main effects induced by this process include protein cross-linking, protein breaks, and modification of side-chain amino acids (Wang et al., 2024). The structural instability of yak fat makes it susceptible to oxidation, and free radicals generated by oxidation promote protein oxidation and destroy amino acids., thus yak meat quality deteriorates and nutritional value is lost (Dong et al., 2023). Consequently, the issue of oxidation-induced deterioration in the quality and safety of meat has attracted considerable attention. It is possible to inhibit the oxidative deterioration of proteins during the manufacture and preservation of meat products by adding antioxidants. Recent studies concentrate on the mechanisms by which antioxidants mitigate MP-mediated oxidation and their ideal application conditions. Consequently, the issue of oxidation-induced deterioration in the quality and safety of meat has been a prominent area of research for some time. During the manufacturing and preservation of meat products, antioxidants can be used to prevent protein oxidation. There has been a shift in focus toward investigating the effects of antioxidants in recent years, including synthetic antioxidants and natural extracts, on the inhibition of MP oxidation and the optimal conditions for their use. A growing number of researchers are directing their attention toward the impact of amino acids on the inhibition of MP oxidation.

Alkaline amino acids, including arginine (Arg), lysine (Lys), and histidine (His), serve as fundamental building blocks of proteins and are classified as essential or conditionally essential amino acids for human nutrition. These amino acids have been industrially synthesized and are recognized for their safety, non-toxicity, availability, nutritional value, and cost-effectiveness, positioning them as green food additives (Deng et al., 2024). In light of these attributes, researchers have been exploring alkaline amino acids as additives to meat products for their antioxidant properties. Arg is an alkaline amino acid widely used in the meat processing industry to improve meat's color and flavor. As a result of advances in meat science, the use of exogenous basic amino acids as polyphosphate substitutes has become a hot topic for research. Chen et al. found that pork quality improved when Arg and Lys were injected into the longissimus dorsi muscle and matured (Chen et al., 2022). Microscopic conformation revealed that Arg helped MP to form a dense and homogeneous three-dimensional network structure, which improved the water retention and hydration capacity of the meat (Zheng et al., 2017). Arg and Lys were found to inhibit lipid and protein oxidation in sausage following previous study (Xu et al., 2018). The aforementioned studies have demonstrated that Arg, either independently or in conjunction with additional additives, can enhance the quality attributes of MP and their derivative products. Despite extensive research on the addition of Arg to meat products, there has been a paucity of research conducted on the effects of Arg on yak meat. Furthermore, the mechanisms through which Arg affects the antioxidant and gel properties of yak MP remain unclear, and the optimal concentration ratio has yet to be determined. Therefore, it is necessary to systematically investigate the effects of Arg on the post-slaughter oxidative and MP gel properties of yak meat based on previous studies. In this study, we investigated how Arg changes the physicochemical properties, protein oxidation, and gel properties of yak meat MP. The study also investigated the correlation between the effects of Arg on the oxidative repair and its changes, internal mechanism of yak meat MP, which could improve the acknowledgement of Arg as an antioxidant to improve meat protein oxidative stability.

2. Materials and methods

2.1. Materials

In the present study, the longissimus dorsi muscle samples (from 12th thoracic vertebrae to 5th lumbar vertebrae) were procured from four robust, disease-free, 3-year-old male yaks at the Jiangnan slaughterhouse in Sichuan, China. Within a half-hour post-slaughter, the muscle tissue was meticulously dissected into approximately 40.0 g cubes. Subsequently, all adipose tissue and connective fascia were meticulously excised. After preparation, the muscle samples were sealed in self-sealing plastic bags and stored at −80 °C for up to 3 months for later analysis. The chemical reagents of analytical grade utilized in this experiment were sourced from Chengdu Kelong Chemical Co., Ltd., located in Chengdu, China.

2.2. MP extraction and sample preparation

2.2.1. Extraction of MP

Weigh 5.0 g of meat sample, add quadruple the volume of extraction solution to homogenize for 30 s. Centrifuge (Eppendorf, PHS-3C, Hamburg, Germany) the sample at 4 °C (15 min, 2000 ×g), discard the supernatant, and repeat the appealing step for three times. Afterwards, the precipitate was dissolved in 4 times the volume of 0.1 mol/L NaCl solution, homogenized, and then filtered through four layers of gauze to remove connective tissue, then centrifuged (4 °C, 15 min, 2000 ×g) to discard the supernatant, and the precipitate was collected to be the MP solution. The concentration of the MP solution was determined using the Biuret method and was subsequently utilized within a 48-h period at 4 °C.

2.2.2. Preparation of Arg-MP system

Various concentrations of Arg were introduced to the MP system to achieve final concentrations of 0.025 %, 0.05 %, 0.10 %, and 0.20 %, respectively. These groups were designated as Arg1, Arg2, Arg3, and Arg4. The control group without the addition of Arg served as the baseline for comparison.

2.3. Solubility

MP was made into a suspension of 2.5 mg/mL with 50.0 mmol/L phosphate buffer, and then centrifuged (2000 ×g, 20 min) for 1 h at 4 °C. The supernatant was taken to determine the protein concentration, and the determination was repeated three times, and the results were averaged.

$$\text{Solubility}\ (\%) = \frac{\text{Supernatant protein content}}{\text{Total protein content}} \quad (1)$$

2.4. Rheological properties

The rheological properties of a 40.0 mg/mL MP solution were evaluated utilizing a rheometer (Discovery HR-1; TA Instruments, New Castle, USA). The temperature scanning mode was adopted. The parameters were set as follows: frequency 0.1 Hz, starting temperature 25 °C, termination temperature 85 °C, temperature increase rate 2 °C/min, strain 0.5 %, and crevice spacing 0.2 mm.

2.5. Preparation of gels

Each of the MP samples was modified to have a mass concentration of 40.0 mg/mL using phosphate buffer (20.0 mmol/L, pH 7.0), heated from 25 °C to 80 °C at a rate of 1 °C/min and held for 20 min, then cooled to 4 °C in an ice-water bath, and stored in a refrigerator at 4 °C overnight (12*h*) until use.

2.6. Strength of gels

The MP gel strength was measured by a TA-XT Plus physical property meter (Stable Micro Systems Ltd., Britain). GMIA mode was selected, the probe was P/0.5, and the parameters were set as follows: pre-test, mid-test, and post-test rates of 1.5, 1.0, 1.0 mm/s, respectively, with an interval of 5 s, a trigger force of 5.0 g, strain trigger type, a compression ratio of 40 % for the sample. All measurements were performed six times to ensure the accuracy of the results.

2.7. Cooking loss and water holding capacity of gels

Determination of gel cooking loss was done by first weighing the MP emulsion before steam treatment (A), then placing the gel in a refrigerator overnight and recording the weight (B) after wiping off the surface moisture.

$$\text{Steaming loss}\ (\%) = \frac{(A-B)}{A} \times 100\%. \tag{2}$$

The water holding capacity (*WHC*) of the gel was determined by cutting the gel into 30.0 × 10.0 × 10.0 mm pieces, placing it in a 10.0 mL centrifuge tube, accurately weighing the weight of the tube as well as the weight of the gel after its addition, centrifuging it at 1000.0 g for 10 min, removing the water, and accurately weighing the remaining weight.

$$\text{WHC}\ (\%) = \frac{\text{The weight of the gel after centrifugation}}{\text{The weight before centrifugation}} \tag{3}$$

2.8. Low field nuclear magnetic resonance (LF-NMR) analysis

In this study, the moisture state and distribution of MP were determined by a nuclear magnetic resonance (NMR) analyzer (Suzhou New Max Analytical Instruments Co., Ltd., Jiangsu, China) according to the method described by (Pereira et al., 2021). The experimental parameters were set as follows: a Carr-Purcell-Meiboom-Gill pulse sequence with a repetition time of 4000.0 ms, acquiring 10,000 echoes across 8 scans. The spin relaxation time (T_2) measurements were conducted at a temperature of 32 °C. Data were graphically represented as relaxation curves, detailing the T_2 values alongside their respective peak magnitudes (A_2) and the ratios of these peak areas (P_2).

2.9. Carbonyl content

The protein carbonyl content was measured using the 2,4-dinitrophenylhydrazine (DNPH) assay, following the procedure described by (Zhang et al., 2020). To 0.5 mL of MP solution, 0.5 mL of 2.0 mol/L HCl solution containing 0.02 mol/L DNPH was added, and 0.5 mL of 2.0 mol/L HCl solution (without DNPH) was added to the control group as well, and the reaction was carried out for 40 min at 25 °C after mixing, and then 2.0 mL of trichloroacetic acid (20 % mass fraction) was added. After mixing and centrifugation (4 °C, 11000 ×*g*, 5 min), the supernatant was discarded, and the precipitate was washed three times with 1.0 mL ethanol: ethyl acetate solution (Volume ratio 1:1), and the precipitate was suspended with 3.0 mL of 6.0 mol/L guanidine hydrochloride solution and kept warm in a water bath for 30 min at 37 °C, and the control group was used as the control.

$$\text{Carbonyl content(nmol/mg)} = \frac{(A_1 - A_0) \times n}{\varepsilon \times \iota \times c} \times 10^6 \tag{4}$$

where: A_1 is the absorbance of the sample, A_0 is the absorbance of the blank control group, n is the dilution factor, ε is the molar absorbance coefficient, ι is the optical path, and c is the mass concentration of MP solution.

2.10. Sulfhydryl (SH) content

Referring to the method of (Li, Zhou, et al., 2023) and adjusted appropriately, the MP solution's concentration was standardized to 2.0 mg/mL. Subsequently, 0.5 mL of this MP solution was incrementally mixed with 2.0 mL of a Urea-Sodium dodecyl sulfate (SDS) solution (comprising 8.0 mol/L urea, 30.0 g/L SDS, and 0.1 mol/L sodium phosphate buffer at pH 7.4) and 0.5 mL of a 10.0 mmol/L DTNB reagent solution (prepared in 0.1 mol/L sodium phosphate buffer at pH 7.4). The control group excluded the DTNB reagent. The reaction was carried out at room temperature for 15 min and absorbance was recorded at 412 nm wavelength using the ultraviolet spectrophotometer (Aoyi, UV-1900, Shanghai, China).

$$\text{SH content}\ (\text{nmol/mg}) = \frac{(A_1 - A_0) \times n}{\varepsilon \times \iota \times c} \times 10^6 \tag{5}$$

where: A_1 is the absorbance of the sample, A_0 is the absorbance of the blank control group, n is the dilution factor, ε is the molar absorbance coefficient, ι is the optical path, and c is the mass concentration of MP solution.

2.11. Surface hydrophobicity

The experimental procedure commenced with the addition of 200.0 μL of a 5.0 mg/mL MP solution to an equal volume of 1.0 mg/mL bromophenol blue (BPB) solution. Another 1.0 mL of 20.0 mmol/L phosphate buffer (pH 6.0) was taken and 200.0 μL of 1.0 mg/mL BPB solution was added. After shaking for 10 min at room temperature, centrifuge at 5000 r/min for 15 min. Subsequently, after the supernatant was diluted 10-fold with phosphate buffer, the absorbance was measured at 595 nm. The surface hydrophobicity is expressed by the binding amount of BPB and calculated according to formula (6).

$$\text{Surface hydrophobicity} \Big/ \mu g = \frac{A_0 - A_1}{A_0} \times 200 \tag{6}$$

A_0 is the absorbance of phosphate buffer solution and A_1 is the absorbance of sample solution.

2.12. Sodium dodecyl sulfate-polyacrylamide gel electrop horesis (SDS-PAGE)

For this experiment, combine 900.0 μL of sample buffer with 5.0 μL of β-mercaptoethanol and 50.0 μL of 1 % bromophenol blue, and incubate for 10 min before cooling to room temperature. Retrieve the pre-chilled marker from −24 °C and allow it to equilibrate to room temperature. Apply 5.0 μL of the marker and 10.0 μL of the test samples. Utilize an electrophoresis apparatus (Liu yi Biotechnology Co., Ltd., DYY-6C, Beijing, China) and initiate the following program: begin at 80 V for 30 min, then increase to 120 V for 120 min. Terminate electrophoresis when the tracking dye is 1.0 cm from the gel's lower edge. Once electrophoresis is halted, remove the gel and immerse it in staining solution for 60 min. Subsequently, distain the gel with decolorizing solution until the background is clear.

2.13. Particle size and zeta-potential

The particle size and zeta potential of the MP were measured using a

particle size analyzer from (Malvern Instruments Ltd., Great Malvern, UK), following the procedures established by (Sun et al., 2024). For particle size measurement, the MP solution at a concentration of 4.0 mg/mL was removed from the measurement background and dispersed in 800 mL of distilled water until the shading reached 10 % to 13 % for measurement. The 1.0 mg/mL MP solution was placed in a quartz cuvette and the zeta-potential was measured at room temperature under the following conditions: scattering angle of 90°, equilibration time of 120 s, and a testing temperature of 25 °C.

2.14. Fluorescence spectroscopy

The MP solution was diluted to 0.5 mg/mL and a fluorescence spectrophotometer was performed prior to analysis with a fluorescence spectrophotometer. The instrument settings were configured with an excitation wavelength of 295 nm using the F-4700 spectrofluorometer (Hitachi, Tokyo, Japan), covering a spectrum from 300 to 400 nm, at a scan rate of 1500 nm/min, and both the emission and excitation slit widths were set to 2.5 nm.

2.15. Fourier transformed infrared spectroscopy (FTIR)

After the concentration of MP was adjusted to 10.0 mg/mL, the sample was freeze-dried for 24 h. After removal, the sample was ground to powder by mortar and pestle, and then measured by Fourier transform infrared spectrometer (PerkinElmer, LR 64912C, Massachusetts, USA). The spectroscopic settings included a scan range from 500.0 to 4000.0 cm^{-1}, a resolution setting of 4.0 cm^{-1}, and the process was repeated 32 times.

2.16. Microstructure of MP gels

The MP gel samples were pretreated, and the gel samples were cut into cubes of 2.0 × 2.0 × 2.0 mm and placed in a fixative with a mass fraction of 2.5 % glutaraldehyde at a low temperature of 4 °C for 48 h. Subsequently, the samples underwent dehydration through sequential immersion in ethanol solutions of 50 %, 70 %, 80 %, and 90 % concentrations for 15 min each, followed by a 15-min treatment with isoamyl acetate. The samples, prepared at varying concentrations, were subjected to freeze-drying and gold sputtering for scanning electron microscopy (Hitachi, SU-8010, Tokyo, Japan), which was conducted at a magnification of 1000 times.

2.17. Statistical analysis

Data calculations were performed utilizing Microsoft Excel 2019, while statistical analyses were conducted with SPSS version 27.0. The determination of statistical significance was based on Duncan's multiple range test at a threshold of $P < 0.05$, indicating a significant difference. Graphical representation of the data was facilitated by Origin Pro 2022 software. All data points are presented as the mean ± standard deviation, derived from triplicate experiments.

3. Results and discussion

3.1. MP functional characteristics

3.1.1. Solubility

MP solubility is a pivotal physicochemical attribute that significantly influences the textural, water retention, and emulsification stability of meat products (Zhou et al., 2022). Protein solubility, a measure of denaturation levels, was observed to peak within the Arg4 group, recording an 88.4 % enhancement in comparison to the control group during our investigation. Fig. 1 (a) illustrates that the MP solubility exhibited an upward trajectory with the augmentation of Arg incorporation, with a notable disparity ($P < 0.05$) when contrasted with the control cohort. This outcome substantiates the adherence to the concentration-dependent pattern. The observed correlation likely arises

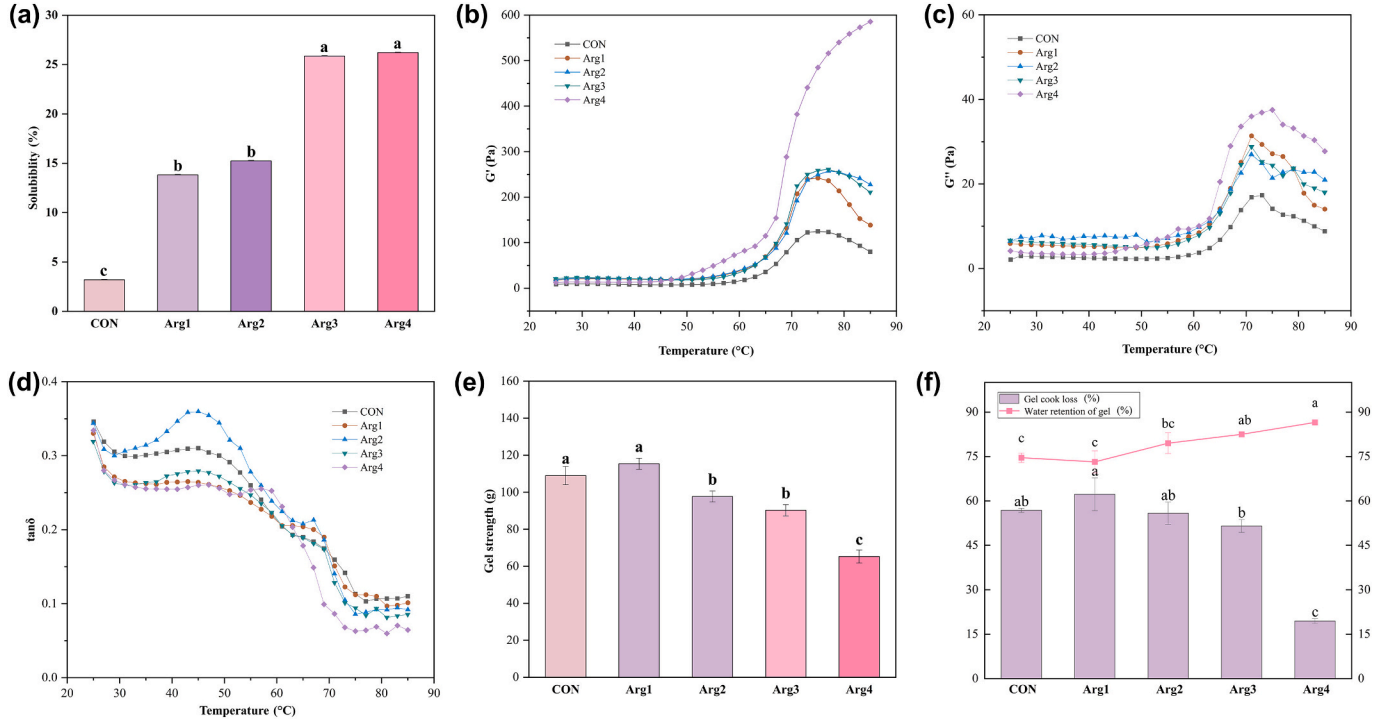

Fig. 1. Effect of Arg on MP solubility **(a)**, energy storage modulus (*G'*, **b)**, loss modulus (*G''*, **c)**, damping factor (tan*δ*, d), MP gel strength **(e)**, gel cooking loss and water retention of gel **(f)** CON: control group (non-treated samples). The symbols Arg1, Arg2, Arg3 and Arg4 represent mixed MP at concentrations of 0.025 %, 0.05 %, 0.10 % and 0.20 %, respectively. Duncan's New Multiple-range test was used to analyze the differences in the six groups respectively. Values of different groups with different lowercase letters (a-e) are significantly different at $P < 0.05$. Error bars were standard errors of the mean ($n = 3$), the same below.

from the characteristic effects of Arg as a basic amino acid, which can prevent myosin clustering, promote protein structure extension, and increase the accessibility of normally hidden binding sites. Furthermore, Arg is suggested to modify the architecture of the protein gel network and exert a pronounced solubilizing effect (Gao et al., 2018).

3.1.2. Rheological properties

The rheological properties of MP play a critical role in assessing their physicochemical properties. The effect of Arg addition on the dynamic rheological properties of MP gels was explored by determining G', G'' and tanδ. The storage modulus, G' reflects the gel network's elasticity and is influenced by temperature, serving as a characteristic of gel structure formation. Conversely, the loss modulus, G'', indicates the energy dissipation due to viscous flow, thereby mirroring the gel's viscous and fluid-like attributes (Sheng et al., 2022). The damping factor tanδ is G''/G', and the sample behaves as a perfectly elastic gel when tanδ value of zero, and as a perfectly viscous gel when tanδ is infinity.

As illustrated in Fig. 1 (b, c), the incorporation of Arg resulted in the rheological behavior of the MP gels exhibiting more solid characteristics. The G' and G'' of all samples in the treatment group exhibited a gradual increase during the warming process from 25 °C to 60 °C. This could be attributed to intermolecular interactions such as ionic and hydrogen bonding (Wu et al., 2024). Upon exceeding 60 °C, the G' and G'' exhibited a sharp increase, indicating the generation of a densely packed gel network. The MP gel G' reached a maximum value (585.619 Pa) when the Arg4 group was at 85 °C. Throughout this procedure, a considerable exposure and interaction of SH and hydrophobic groups occurred, culminating in protein aggregation and the establishment of a gel network. The observed transition of the MP solution from a viscous liquid to a solid state of viscoelasticity was marked by the initial formation of an insoluble mesh-like gel structure.

The effects of different Arg additions on the tanδ values during MP gelation are shown in Fig. 1 (d). The trend was roughly similar among the treatment groups with Arg additions, with an overall sustained increase from 35 to 45 °C, reaching a peak at about 50 °C followed by a sharp decrease with the increase in temperature. This indicates that viscosity dominates the gel system at 35 to 45 °C, while elasticity dominates the gel system after 50 °C. It is noteworthy that the tanδ value of Arg2 group exhibited a continuous increase from 33 to 45 °C, reaching a peak (0.359) at approximately 45 °C. Thereafter, it exhibited a sharp decline with increasing temperature. This suggests that Arg2 group significantly altered the MP system, enhancing its viscoelasticity during the gelation process.

3.2. Gel characteristics

3.2.1. Gel strength

The gelation of MP is a significant quality characteristic of meat products. Gel strength is an important reflection of the ability of MP to form cohesive network structures (Zheng et al., 2019). Fig. 1 (e) illustrates that the incorporation of Arg into the system led to a promotion of the oxidation-induced weakening of the gel. With the addition of Arg, the gel strength exhibited a gradual decline that was dose-dependent. Notably, within the Arg4 group, the gel strength was substantially diminished to 65.26 g, significantly below the control group levels ($P < 0.05$). This finding aligns with the results previously documented by (Peng et al., 2021). The observed outcome may be attributed to Arg's capacity to enhance the MP's fracture index, thereby disrupting the gel's structural integrity and consequently reducing its strength.

3.2.2. Cooking loss and water retention of gel

The cooking loss and the water retention of thermogenic gels are indicative of their capacity to bind water (Lian et al., 2023). The cooking loss enables an evaluation of the emulsification stability of the MP gel. The water-holding capacity is a critical parameter for evaluating the interactions between proteins and their aqueous environment. Additionally, it provides insight into the overall roughness of the protein gel structure, which is a significant factor in assessing gel quality. As depicted in Fig. 1 (f), an increment in Arg content correlated with a decrease in cooking loss and an improvement in water retention, indicating a concentration-dependent effect. The Arg4 group demonstrated the most significant reduction in cooking loss ($P < 0.05$), attaining the lowest recorded value of 19.46 %. This was 68.75 % lower than the control group. Additionally, a significant ($P < 0.05$) increase in water retention was observed, reaching a peak value of 86.5 %. This was 18.17 % higher than the control group. These findings are consistent with those of (Fan et al., 2024). This evidence indicates that Arg facilitates the hydrolysis of MP and the subsequent loss of water and gelation of the resulting peptides.

3.2.3. LF-NMR analysis

Low-field nuclear magnetic resonance (LF-NMR) provides insights into the distribution, movement, and binding ability of water within gels through T_2 signal analysis, where a prolonged T_2 signifies greater water mobility and freedom within the system. T_{21} corresponds to the tightly associated water molecules that are closely bound to macromolecules. T_{22} pertains to the water that is partially integrated within the protein's network structure, often referred to as fixed water. In contrast, T_{23} denotes the free water, situated beyond the bounds of the protein matrix. (Chen et al., 2021). Peak area (A_2) and peak area ratio (P_2) are shown in Fig. 2 (a) and summarized in Table 1. The Arg concentration significantly influenced the quantities of A_{21} and A_{22}, with each exhibiting a substantial rise across all experimental groups in contrast to the control. The observed increase achieved statistical significance ($P < 0.05$) with elevated concentrations of Arg. These results further validate the potential of Arg supplementation in enhancing protein-water interactions, with the Arg2 group demonstrating the highest P_{22} value, showing a 1.12 % increase relative to the control group. This outcome indicates a significantly higher proportion of fixed water, which contributes to the observed experimental findings. The enhancement of protein-water bonding is likely due to the elevated Arg levels, resulting in a rise in disulfide bond formation and a reduction in hydrophobic interactions. Consequently, this led to the development of a more compact gel matrix in the samples, corroborating the results reported by (Jiang et al., 2023). It is notable that the concentration of Arg was found to have a significant impact on the formation of A_{23}, with an increase observed at higher Arg concentrations ($P < 0.05$). Nonetheless, the P_{23} peak area ratio remained statistically unchanged with escalating Arg concentrations relative to the control group ($P > 0.05$), suggesting that the gel's overall water distribution and retention capabilities were not markedly influenced. LF-NMR analysis of the sample gels further validated the impact of Arg in promoting a more stable gel structure and the encapsulation of water molecules. This stabilization, in turn, diminished water mobility, consequently enhancing the gel's water retention capacity.

3.3. MP oxidation level

3.3.1. Carbonyl content

The carbonyl content serves as a key indicator for evaluating alterations in the primary protein structure and the extent of MP oxidation. (Li et al., 2021). As depicted in Fig. 2 (b), the carbonyl content exhibited a significant reduction in the Arg-supplemented group compared to the control ($P < 0.05$), potentially attributed to Arg's capacity to neutralize free radicals and form complexes with metal ions, it is worthwhile to pay attention to the fact that the carbonyl content tended to increase with the increase of the content of Arg. However, all values remained below those of the control group, possibly because protein oxidation typically involves the modification of amino acid side chains. The oxidation of Arg resulted in the generation of carbonyl groups, a process that can lead to the degradation of the MP gel structure and a consequent decrease in gel strength. (Pan, Bai, et al., 2023), as evidenced by the findings presented in Fig. 1 (e). It can be observed that Arg exerts an inhibitory effect

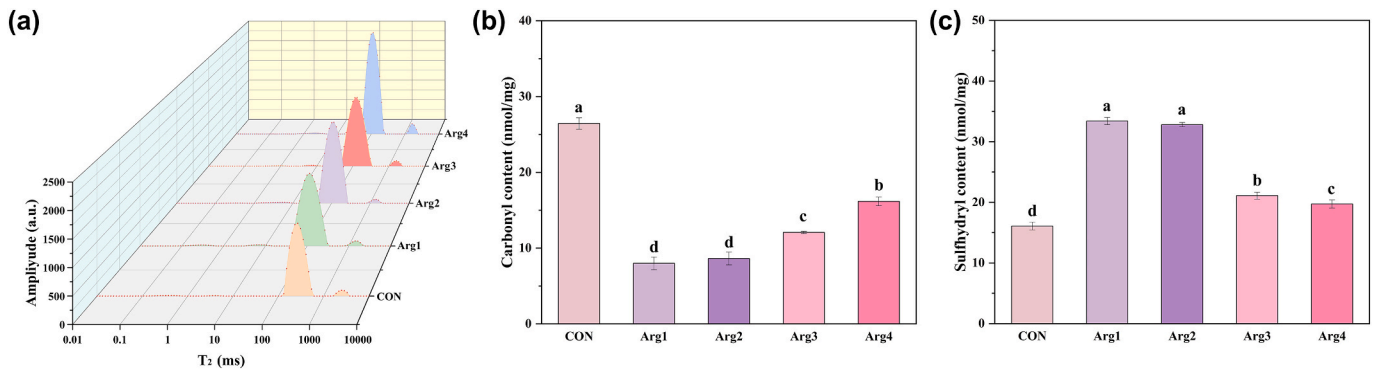

Fig. 2. Effect of Arg on MP moisture distribution status **(a)**, carbonyl content **(b)**, sulfhydryl content**(c)**. CON: control group (non-treated samples). The symbols Arg1, Arg2, Arg3 and Arg4 represent mixed MP at concentrations of 0.025 %, 0.05 %, 0.10 % and 0.20 %, respectively.

Table. 1
Effect of different concentrations of Arg on MP gel area of strongly bound water (A_{2b}), bound water (A_{21}), fixed water (A_{22}), free water peak (A_{23}) and the proportion of strongly bound water (P_{2b}), bound water (P_{21}), fixed water (P_{22}), free water peak (P_{23}). CON: control group (non-treated samples). The symbols Arg1, Arg2, Arg3 and Arg4 represent mixed MP at concentrations of 0.025 %, 0.05 %, 0.10 % and 0.20 %, respectively. Duncan's New Multiple-range test was used to analyze the differences in the six groups respectively ($P < 0.05$), the significances were showed in the present study. Error bars were standard errors of the mean (n = 3).

	A21	*A22*	*A23*	*P21*	*P22*	*P23*
CON	109.36 ± 8.62^{c}	8839.18 ± 112.00^{d}	365.81 ± 44.48^{d}	1.17 ± 0.08^{c}	94.90 ± 0.52^{b}	3.92 ± 0.46^{ab}
Arg1	205.64 ± 14.51^{b}	$13,104.71 \pm 317.91^{c}$	510.46 ± 84.94^{c}	1.45 ± 0.129^{b}	94.92 ± 0.83^{b}	3.62 ± 0.74^{b}
Arg2	213.33 ± 1.88^{b}	$13,326.34 \pm 581.99^{c}$	337.85 ± 28.21^{d}	1.53 ± 0.071^{b}	96.02 ± 0.37^{a}	2.44 ± 0.30^{c}
Arg3	255.93 ± 10.37^{a}	$14,103.41 \pm 334.55^{b}$	629.07 ± 21.00^{b}	1.70 ± 0.041^{a}	94.09 ± 0.06^{b}	4.19 ± 0.04^{ab}
Arg4	266.45 ± 0.091^{a}	$17,121.57 \pm 113.58^{a}$	809.53 ± 32.80^{a}	1.46 ± 0.007^{b}	94.09 ± 0.21^{b}	4.44 ± 0.20^{a}

on MP activity; however, this effect is concentration-dependent. Excessive Arg concentrations may, in fact, stimulate MP oxidation.

3.3.2. SH content

SH are integral to the stabilization of the tertiary structure of proteins and can serve as indicators of alterations within this structure. The oxidation of proteins can be inferred from the depletion of SH groups. Concurrently, as the oxidation of SH progresses, there is a corresponding increase in the formation of disulfide bonds, which are the oxidation byproducts, while the concentration of SH groups diminishes. (He et al., 2018). Fig. 2 (c) illustrates a statistically significant elevation ($P < 0.05$) in SH content across all groups relative to the control group. This increase might be attributed to Arg's inhibitory role in the transformation of SH groups into intramolecular and intermolecular disulfide bonds and its neutralization of other oxidizing agents, thereby exerting an antioxidant effect on MP. As Arg content rose, a downward trend in SH content was observed. This could be due to the increased amino group count in the myofibrillar MP hydrolysate following Arg addition, which likely facilitated MP solubility expansion, making the oxidation-prone SH groups more accessible, consequently leading to a reduction in SH content (Zhang, Wu, et al., 2022). It can be concluded that Arg exerts an inhibitory effect on MP oxidation, which is consistent with the results obtained from the carbonyl content.

3.3.3. Surface hydrophobicity

The surface hydrophobicity of a protein mirrors its conformational shifts and correlates with the extent to which hydrophobic areas are exposed on the protein's surface (Cao et al., 2023). Protein oxidative denaturation prompts the unraveling of their molecular architecture, unveiling hydrophobic amino acids that were initially concealed, consequently elevating the protein's surface hydrophobicity. Fig. 3 (a) demonstrates a significant reduction in surface hydrophobicity with escalating Arg supplementation ($P < 0.05$). This reduction may be attributed to Arg's protective role against oxidative damage to the protein structure. As a result, the increased net surface charge could mitigate protein oxidation. The enhanced charge on MP can, in turn, strengthen the interaction with water, which is advantageous for retaining water and reducing the extent of MP denaturation. This result is supported by the water retention measurements of the gels, as illustrated in Fig. 1 (f).

3.3.4. SDS-page

The impact of varying Arg concentrations on the MP fractions was evaluated using sodium dodecyl SDS-PAGE. Fig. 3 (b) presents the SDS-PAGE profiles of MP spanning molecular weights from approximately 10 to 180 kDa. A prominent band indicative of the myosin heavy chain, exceeding 180 kDa in molecular weight, was identified. Additionally, a band corresponding to actin, with a molecular weight of approximately 40 kDa, was also observed. Concurrently, bands of lower intensity, corresponding to molecular weights of 35, 25, and 15 kDa, were noted across all samples (Jiao et al., 2024). These bands may be due to moderate oxidation induced by the addition of Arg, which promotes cross-linking between the MP molecules or assemblies to form high molecular weight bands. With escalating Arg content relative to the control group, there was a gradual increase in the grayscale values of bands corresponding to molecular weights of 35, 25, and 15 kDa. This increase might be attributed to the degradation of larger molecules into smaller proteins, peptides, or even amino acids following the appropriate oxidation of the proteins (Pan, Ma, et al., 2023).

3.4. Particle size

Protein aggregation levels are mirrored by variations in the average particle diameter. Overall, the processes of protein aggregation and denaturation are associated with an enlargement of protein particle dimensions (Zhao et al., 2024). As illustrated in Fig. 3 (c), the gradual increase in Arg content resulted in a trend of decreasing and then increasing average overall particle size of MP d (4, 3) and average size of face particles d (3,2), reaching a nadir at Arg2 group compared to the control group. Specifically, d (4, 3) decreased by 26.53 % and d (4, 3) decreased by 38.45 %. This is consistent with the result of (Zhang, Wu, et al., 2022). This phenomenon may be attributed to the alkaline

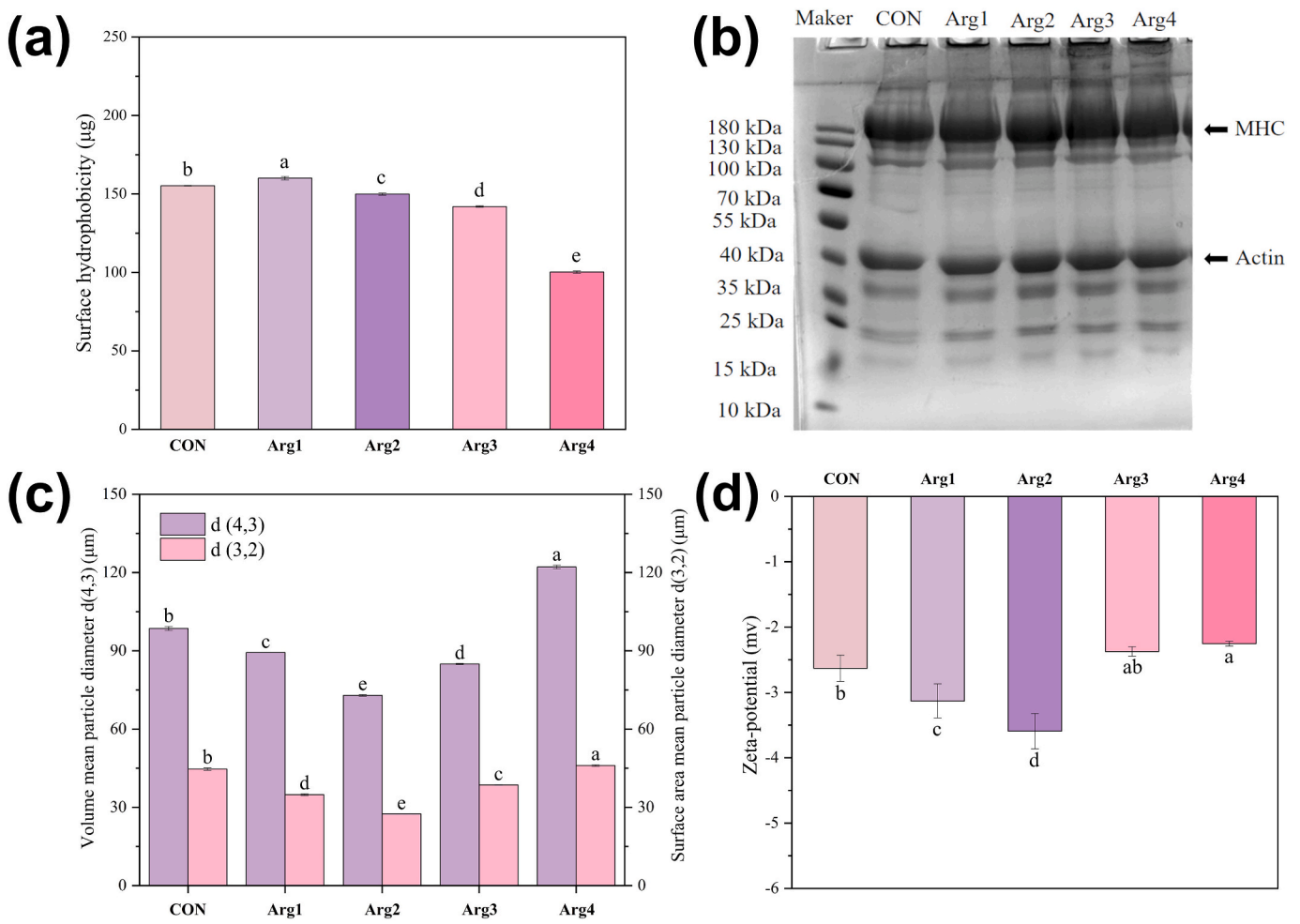

Fig. 3. Effect of Arg on MP surface hydrophobicity **(a)**, SDS-PAGE of MPs treated with different Arg concentrations **(b)**, particle size **(c)**, Zeta-potential **(d).** CON: control group (non-treated samples). The symbols Arg1, Arg2, Arg3 and Arg4 represent mixed MP at concentrations of 0.025 %, 0.05 %, 0.10 % and 0.20 %, respectively. Marker: protein marker (molecular weight of standard).

environment provided by Arg, which has been demonstrated to lead to the unfolding of microtubules and the depolymerization of MP, resulting in a decrease in the particle size of the Arg-MP complexes. As the Arg content increased, the average particle size of Arg3 group and Arg4 group exhibited an upward trend. Additionally, the Arg4 group exhibited a 19.18 % increase in d (4, 3) compared to the control group, and d (3, 2) showed a 3.98 % elevation. These results suggest that the mean particle size of the MP was adversely affected compared to the control group. It can be hypothesized that the addition of Arg facilitates the oxidation-induced unfolding of the MP structure, thereby allowing the exposure of SH and hydrophobic groups. This process likely facilitated the strengthening of intermolecular disulfide linkages and hydrophobic attractions among protein molecules. This resulted in protein aggregation through intermolecular cross-linking and an associated increase in particle size.

3.5. Zeta-potential

The zeta potential reflects the electric potential magnitude within the protein solution, where higher absolute values indicate greater MP stability. In Fig. 3 (d), negative zeta potential values were observed across all samples due to the inherent negative surface charge of MP. The absolute zeta potential initially increased with Arg addition, peaking in the Arg1 and Arg2 groups ($P < 0.05$), and then declined. The Arg2 group demonstrated the highest absolute potential (3.59 mV). This increase is likely due to Arg's net positive charge, which can counteract the myosin molecules' total net negative charge, especially as the pH shifts away from the isoelectric point following Arg addition. (Shi et al., 2020).

3.6. MP structures

3.6.1. Fluorescence spectroscopy

Protein oxidation unveils tryptophan residues that are typically concealed, consequently diminishing the fluorescence intensity. This approach was utilized to assess the conformational alterations and oxidation extent of MP. The endogenous fluorescence profiles of tryptophan residues were determined to achieve this objective (Li et al., 2019). As depicted in Fig. 4 (a), the fluorescence intensity of MP peaks with increasing Arg concentration, reaching a maximum at Arg3 (181.07 a.u.), a 12.91 % enhancement over the control group. A slight decrease at Arg4 suggests a concentration-dependent antioxidant effect of Arg on MP, potentially limited at higher concentrations. It can be observed that Arg effectively inhibited the change of tertiary structure caused by protein oxidation, leading to aggregation. Previous research has indicated that supplementing duck MP with Arg can significantly prevent the fluorescence intensity decline during freeze-thaw processes, thus preserving the integrity of its tertiary structure. (Li, Zong, et al., 2023). This outcome aligns with the observations of surface hydrophobicity changes.

3.6.2. FTIR

The MP was analyzed by Fourier transform infrared spectrometer

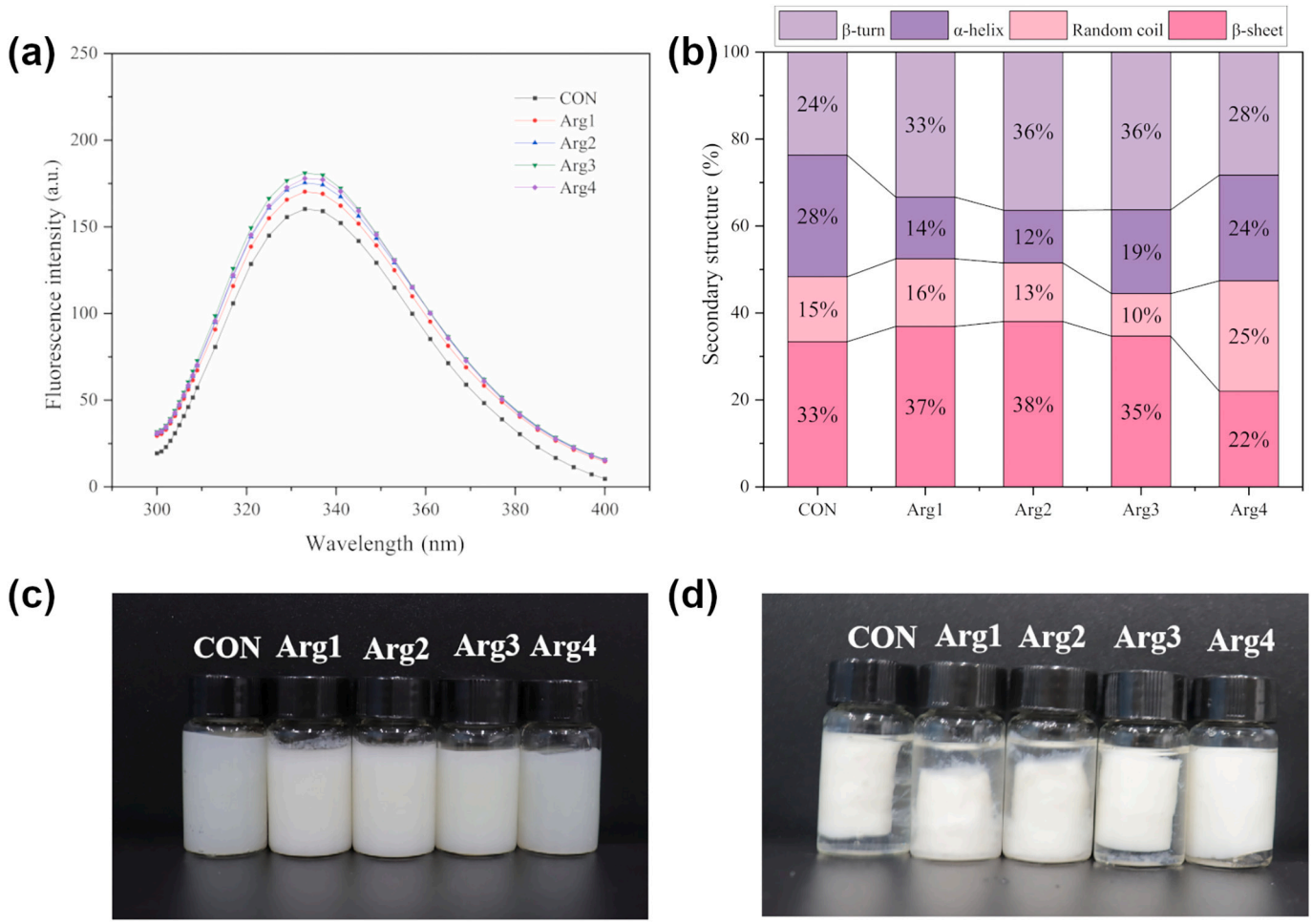

Fig. 4. Effect of Arg on MP intrinsic tryptophan fluorescence spectroscopy **(a)**, fourier transform infrared spectroscopy **(b)** and effect of Arg on the appearance of MP **(c)**, gel **(d).** CON: control group (non-treated samples). The symbols Arg1, Arg2, Arg3 and Arg4 represent mixed MP at concentrations of 0.025 %, 0.05 %, 0.10 % and 0.20 %, respectively.

with full-band scanning (400–4000 cm^{-1}), in which the peaks of 1600–1700 cm^{-1} represent the amide I band, which is mainly induced by the telescopic vibration of C═O and C—N (Zhang et al., 2016). This band can reflect the process of the secondary structure change of the protein. The secondary structure composition of the MP was determined through deconvolution and double integration, as depicted in Fig. 4 (b). As demonstrated in the figure, the control group exhibited 24 %, 28 %, 15 % and 33 % of β-turns, α-helices, random coil and β-sheet, respectively. Upon incrementing Arg levels, the α-helix content in the samples displayed an initial decline followed by an ascent, with all measurements being significantly lower than those of the control group. Specifically, in the Arg2 group, the α-helix content reached its minimum, registering a 16 % reduction compared to the control. The observed phenomenon could be due to the electrostatic repulsion effects of Arg, causing the MP to unfold, and consequently reducing the α-helix content. This is also consistent with the experimental results of (Huang et al., 2021) who used ultrasound and L-Ly/L-Arg to investigate the improvement of the physical stability of myosin-soybean oil emulsions.

In comparison to the control group, the β-sheet content exhibited an increase followed by a decrease, notably peaking in the Arg2 group at a significant level higher than the control ($P < 0.05$), reaching a maximum of 38 %. This elevation implies that Arg may intensify the secondary structural transitions of MP, particularly involving α-helix and β-sheet formations. β-sheet is more ordered than α-helix in the secondary structure of proteins, but β-sheet is more stable than α-helix, so the addition of Arg contributes more to the formation of more stable MP.

3.7. MP gel morphology and microstructure

Fig. 4 (c, d) show the gel state of yak MP gel in the control group and the Arg treatment group before and after heat treatment. It can be seen that the gel structure of Arg1 group is unstable, the water loss rate is large, and the texture is loose and rough. The inability to form a robust gel network structure may be attributed to the reduced solubility of MP and its tendency to aggregate and degenerate following oxidation. With escalating Arg concentration, the gel volume in the Arg1-Arg4 groups progressively expanded, their surfaces evolving to a smoother and finer texture, correlating with a reduction in water loss throughout the cooking process. Meanwhile, the appearance of the gels under a 1000× scanning electron microscope is shown in Fig. 5 (a, b, c, d, e). As the concentration of Arg increased, the gel network exhibited enhanced uniformity and regularity, accompanied by a notable reduction in the size of protein aggregate particles. This resulted in a more compact gel network system, characterized by the elimination of a substantial number of pores and gaps. This also explains that the addition of Arg effectively improved the oxidation-induced reduction of cooking loss.

3.8. Correlation analysis

The interplay among the physicochemical attributes, gel integrity, and oxidation extent of Arg-treated Yak MP was evaluated using Pearson's correlation analysis, with the findings depicted in Fig. 6 (a). The findings indicated an inverse relationship between gel strength and

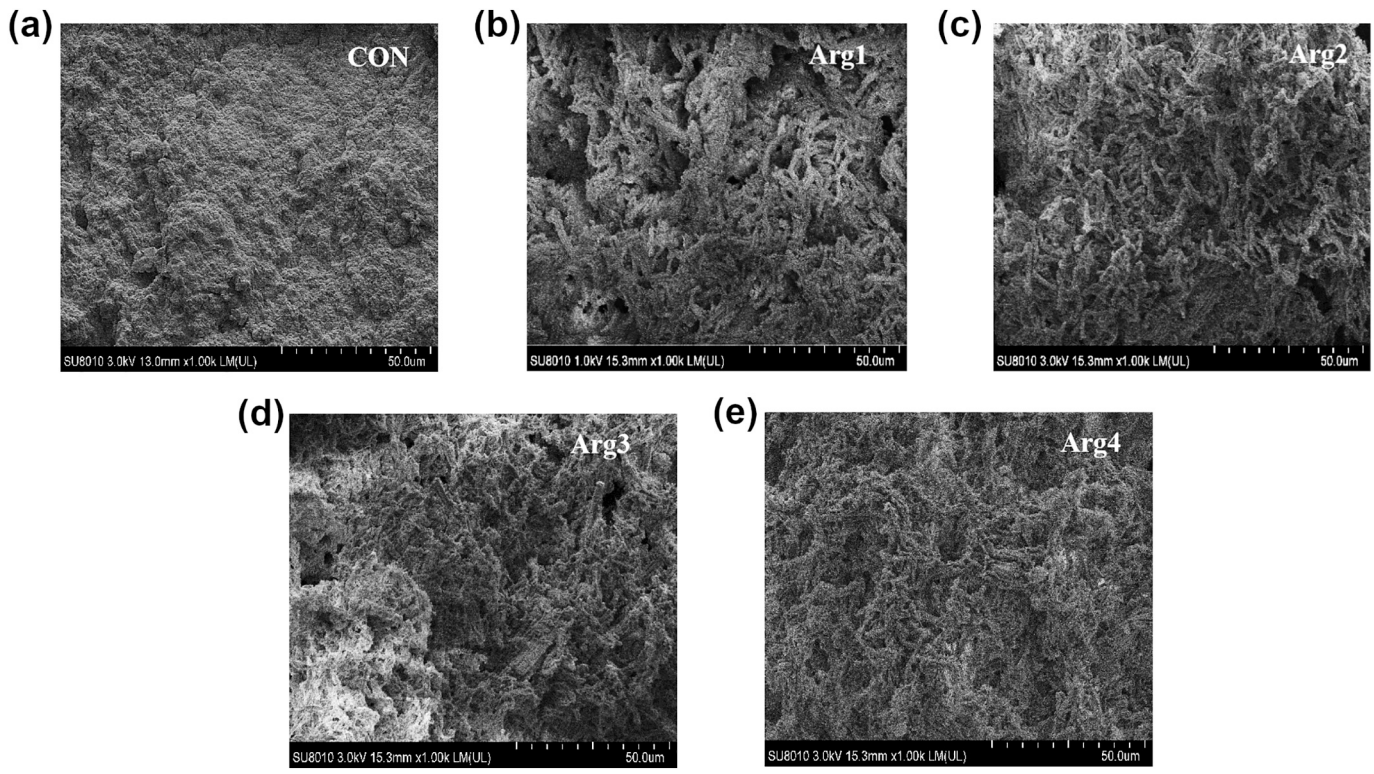

Fig. 5. The observation of different concentrations of Arg on the microstructure of MP gels **(a, b, c, d, e)**. CON: control group (non-treated samples). The symbols Arg1, Arg2, Arg3 and Arg4 represent mixed MP at concentrations of 0.025 %, 0.05 %, 0.10 % and 0.20 %, respectively.

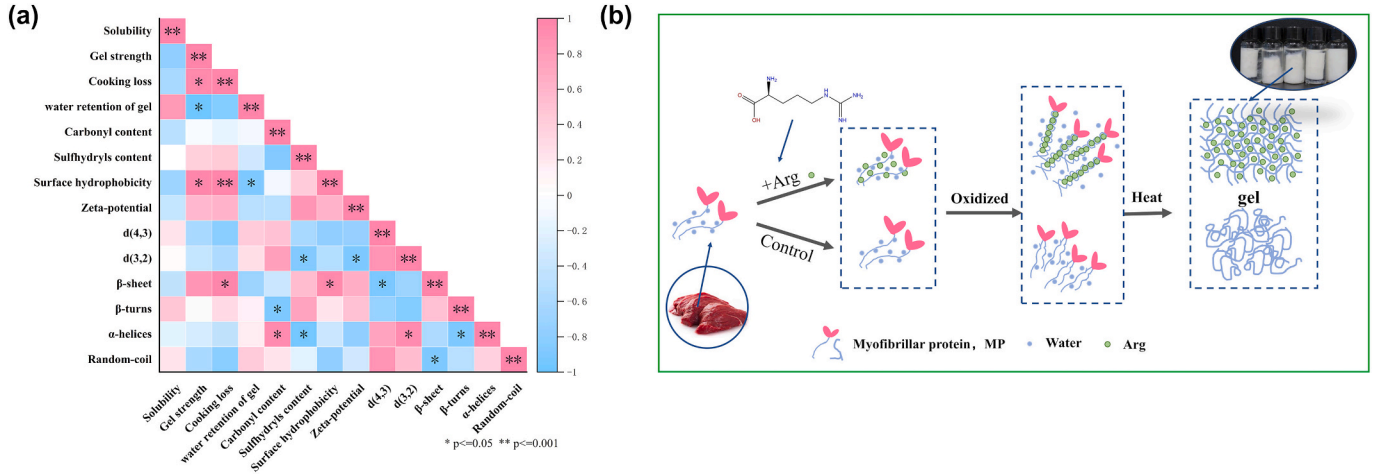

Fig. 6. Correlation analysis between indicators of the effect of Arg on MP **(a)**. Mechanisms by which Arg repairs oxidative damage to MP and improves gel properties **(b)**.

water retention capacity, a notable direct correlation linking cooking loss to gel strength, and a markedly positive association between surface hydrophobicity and β-sheet content. Carbonyl content demonstrated a significant negative correlation with β-turn and a significant positive correlation with α-helices. SH content exhibited a negative correlation with α-helices. SH content demonstrated a significant positive correlation with β-sheet. The particle size parameter d (3, 2) was found to have an inverse relationship with zeta potential while showing a positive linkage with α-helices. Additionally, β-sheets were negatively correlated with random coils, and a similar inverse correlation was noted between β-turns and α-helices.

3.9. Mechanism of Arg action on MP

Fig. 6 (b) delineates the mechanism through which Arg repairs oxidatively damaged MP and augments gel performance. Oxidation significantly diminishes the solubility and stability of MP, leading to the formation of protein aggregates that impede the development of a hydrophilic gel network. Consequently, this results in a disordered gel structure with reduced density, culminating in suboptimal gel performance. The incorporation of Arg induced a structural transition from an initially non-dense and disordered state to a uniform network. The hydrogen bonding between MP and Arg strengthened the binding affinity of MP for water, facilitating the conversion of immobile water into bound water within the gel matrix. As detailed in Table 1, the Arg-MP

mixture enhanced the homogeneity and regularity of the gel network. Additionally, the protein aggregates exhibited a reduction in particle size, as depicted in Fig. 3 (c). This refined and homogeneous mesh structure contributed to the improved texture and water retention of the gels. In conclusion, Arg was found to ameliorate the adverse impacts of oxidation on the physical and functional attributes of MP gels.

4. Conclusion

In this study, Arg displayed significant antioxidant properties against yak MP oxidation, promoting gel network formation and bolstering MP stability. It is important to highlight that the impact of Arg on MP is concentration-dependent. While optimal oxidation promotes gel structure formation, excessive Arg concentrations exceeding 0.05 % can intensify MP oxidation, thereby diminishing gel strength. Intriguingly, the absence of Arg or its minimal presence has been observed to exert a beneficial influence on MP oxidation. Notably, at the 0.05 % concentration (Arg2 group), there was a marked enhancement in various parameters, including water distribution, oxidation levels, particle dimensions, and protein secondary structure, indicating improved overall protein attributes. Additionally, Arg presence in the meat matrix was found to induced the unfolding of MP, fostering the development of a more stable MP structure, which in turn, promoted the establishment of a tighter gel network. The findings suggest that Arg holds promise as an antioxidant in meat processing. However, further research is warranted to determine the optimal concentration range. Subsequent studies should endeavor to dissect the underlying mechanisms and investigate the potential applications of Arg in the context of yak beef myofibrillar protein gels.

CRediT authorship contribution statement

Yuqi Wang: Writing – original draft, Investigation, Formal analysis, Data curation, Conceptualization. **Yiwen Mei:** Writing – review & editing, Data curation. **Rongsheng Du:** Investigation. **Shulin Zhang:** Writing – review & editing. **Qiuyu Wang:** Writing – review & editing. **Xiaofang Dao:** Writing – review & editing. **Na Li:** Writing – review & editing. **Linlin Wang:** Writing – review & editing, Project administration, Funding acquisition. **Honghong He:** Writing – review & editing.

Declaration of competing interest

The authors declare that they have no known competing financial interests or personal relationships that could have appeared to influence the work reported in this paper.

Data availability

Data will be made available on request.

Acknowledgments

We would like to thank the following groups for providing special funds for this research: National Natural Science Foundation of China (No. 32001726); The Natural Science Foundation of Xinjiang Uygur Autonomous Region (No. 2021D01A75).

References

Bu, X., Wang, H., Wang, Y., Ojangba, T., Nan, H., Zhang, L., & Yu, Q. (2023). Effects of iron-catalyzed oxidation and methemoglobin oxidation systems on endogenous enzyme activity and myofibrillar protein degradation in yak meat. *Food Chemistry, 404*, Article 134647. https://doi.org/10.1016/j.foodchem.2022.134647

Cao, C., Zhu, Z., Liang, X., Kong, B., Xu, Z., Shi, P., & Liu, Q. (2023). Elucidation of interactions between myofibrillar proteins and κ-carrageenan as mediated by NaCl level: Perspectives on multiple spectroscopy and molecular docking. *International Journal of Biological Macromolecules, 248*, Article 125903. https://doi.org/10.1016/j.ijbiomac.2023.125903

Chen, H., Zhang, M., & Yang, C. (2021). Comparative analysis of 3D printability and rheological properties of surimi gels via LF-NMR and dielectric characteristics. *Journal of Food Engineering, 292*, Article 110278. https://doi.org/10.1016/j.jfoodeng.2020.110278

Chen, L., Bao, P., Wang, Y., Hu, Y., Fang, H., Yang, H., & Zhou, C. (2022). Improving quality attributes of refrigerated prepared pork chops by injecting l-arginine and l-lysine solution. *LWT, 153*, Article 112423. https://doi.org/10.1016/j.lwt.2021.112423

Deng, P., Teng, S., Zhou, Y., Liu, Y., Liao, B., Ren, X., & Zhang, Y. (2024). Effects of basic amino acids on heterocyclic amines and quality characteristics of fried beef patties at low NaCl level. *Meat Science, 215*, Article 109541. https://doi.org/10.1016/j.meatsci.2024.109541

Dong, K., Guan, Y., Wang, Q., Huang, Y., An, F., Zeng, Q., & Huang, Q. (2023). Non-destructive prediction of yak meat freshness indicator by hyperspectral techniques in the oxidation process. *Food Chemistry: X, 17*, Article 100541. https://doi.org/10.1016/j.fochx.2022.100541

Fan, X., Gao, X., Li, R., Pan, D., & Zhou, C. (2024). Myofibrillar proteins' intermolecular interaction weakening and degradation: Are they mainly responsible for the tenderization of meat containing l–arginine, l-lysine, or/and NaCl? *Food Chemistry, 441*, Article 138318. https://doi.org/10.1016/j.foodchem.2023.138318

Gao, R., Wang, Y., Mu, J., Shi, T., & Yuan, L. (2018). Effect of l-histidine on the heat-induced aggregation of bighead carp (Aristichthys nobilis) myosin in low/high ionic strength solution. *Food Hydrocolloids, 75*, 174–181. https://doi.org/10.1016/j.foodhyd.2017.08.029

Grasso, S., Estévez, M., Lorenzo, J. M., Pateiro, M., & Ponnampalam, E. N. (2024). The utilisation of agricultural by-products in processed meat products: Effects on physicochemical, nutritional and sensory quality – Invited review. *Meat Science, 211*, Article 109451. https://doi.org/10.1016/j.meatsci.2024.109451

Gu, Z. (2024). Male yaks adapt to heat stress with enhancement of immunomodulation, anti-oxidation, and blood oxygen delivery. *Journal of Thermal Biology*. , Article 103879. https://doi.org/10.1016/j.jtherbio.2024.103879

Guo, Z., Ge, X., Yang, L., Ma, G., Ma, J., Yu, Q., & Han, L. (2021). Ultrasound-assisted thawing of frozen white yak meat: Effects on thawing rate, meat quality, nutrients, and microstructure. *Ultrasonics Sonochemistry, 70*, Article 105345. https://doi.org/10.1016/j.ultsonch.2020.105345

He, Y., Huang, H., Li, L., Yang, X., Hao, S., Chen, S., & Deng, J. (2018). The effects of modified atmosphere packaging and enzyme inhibitors on protein oxidation of tilapia muscle during iced storage. *LWT, 87*, 186–193. https://doi.org/10.1016/j.lwt.2017.08.046

Huang, Y., Zhang, D., Zhang, Y., Fang, H., & Zhou, C. (2021). Role of ultrasound and l-lysine/l-argnine in improving the physical stability of myosin-soybean oil emulsion. *Food Hydrocolloids, 111*, Article 106367. https://doi.org/10.1016/j.foodhyd.2020.106367

Jiang, Q., Chen, N., Gao, P., Yu, D., Yang, F., Xu, Y., & Xia, W. (2023). Influence of L-arginine addition on the gel properties of reduced-salt white leg shrimp (Litopenaeus vannamei) surimi gel treated with microbial transglutaminase. *LWT, 173*, Article 114310. https://doi.org/10.1016/j.lwt.2022.114310

Jiao, X., Li, X., Zhang, N., Yan, B., Huang, J., Zhao, J., & Fan, D. (2024). Solubilization of fish myofibrillar proteins in NaCl and KCl solutions: A DIA-based proteomics analysis. *Food Chemistry, 445*, Article 138662. https://doi.org/10.1016/j.foodchem.2024.138662

Li, F., Du, X., Ren, Y., Kong, B., Wang, B., Xia, X., & Bao, Y. (2021). Impact of ice structuring protein on myofibrillar protein aggregation behaviour and structural property of quick-frozen patty during frozen storage. *International Journal of Biological Macromolecules, 178*, 136–142. https://doi.org/10.1016/j.ijbiomac.2021.02.158

Li, F., Wang, B., Kong, B., Shi, S., & Xia, X. (2019). Decreased gelling properties of protein in mirror carp (Cyprinus carpio) are due to protein aggregation and structure deterioration when subjected to freeze-thaw cycles. *Food Hydrocolloids, 97*, Article 105223. https://doi.org/10.1016/j.foodhyd.2019.105223

Li, J., Zhou, Y., Li, Z., Ma, Z., Ma, Q., & Wang, L. (2023). Mechanism for improving the gel properties of transglutaminase-mediated porcine myofibrillar protein by ultrasonic pretreatment combined with carrageenan. *Food Chemistry, 426*, Article 136635. https://doi.org/10.1016/j.foodchem.2023.136635

Li, M., He, S., Sun, Y., Pan, D., Zhou, C., & He, J. (2023). Effectiveness of l-arginine/l-lysine in retarding deterioration of structural and gelling properties of duck meat myofibrillar protein during freeze-thaw cycles. *Food Bioscience, 51*, Article 102302. https://doi.org/10.1016/j.fbio.2022.102302

Li, Y., Zong, W., Zhao, S., Qie, M., Yang, X., & Zhao, Y. (2023). Nutrition and edible characteristics, origin traceability and authenticity identification of yak meat and milk: A review. *Trends in Food Science & Technology, 139*, Article 104133. https://doi.org/10.1016/j.tifs.2023.104133

Lian, F., Cheng, J., Wang, H., & Sun, D. (2023). Effects of combined roasting and steam cooking on NaCl reduction and quality changes in marinated salmon flesh as compared with roasting and water bath cooking. *LWT, 179*, Article 114623. https://doi.org/10.1016/j.lwt.2023.114623

Pan, D., Ma, J., Diao, J., Li, J., & Chen, H. (2023). Effects of eugenol on the structure and gelling properties of myofibrillar proteins under hydroxyl radical-induced oxidative stress. *Food Chemistry: X, 20*, Article 100946. https://doi.org/10.1016/j.fochx.2023.100946

Pan, N., Bai, X., Kong, B., Liu, Q., Chen, Q., Sun, F., & Xia, X. (2023). The dynamic change in the degradation and in vitro digestive properties of porcine myofibrillar protein during freezing storage. *International Journal of Biological Macromolecules, 234*, Article 123682. https://doi.org/10.1016/j.ijbiomac.2023.123682

Peng, Z., Zhang, Y., Wang, H., Gao, G., Yu, Z., Chong, P. H., & Wang, Q. (2021). Effects of arginine-glucose Maillard reaction products on the physicochemical and gel

properties of chicken myofibrillar protein. *LWT, 152*, Article 112244. https://doi.org/10.1016/j.lwt.2021.112244

Pereira, J., Sathuvan, M., Lorenzo, J. M., Boateng, E. F., Brohi, S. A., & Zhang, W. (2021). Insight into the effects of coconut kernel fiber on the functional and microstructural properties of myofibrillar protein gel system. *LWT, 138*, Article 110745. https://doi.org/10.1016/j.lwt.2020.110745

Sheng, L., Liu, Q., Dong, W., & Cai, Z. (2022). Effect of high intensity ultrasound assisted glycosylation on the gel properties of ovalbumin: Texture, rheology, water state and microstructure. *Food Chemistry, 372*, Article 131215. https://doi.org/10.1016/j.foodchem.2021.131215

Shi, T., Xiong, Z., Jin, W., Yuan, L., Sun, Q., Zhang, Y., & Gao, R. (2020). Suppression mechanism of l-arginine in the heat-induced aggregation of bighead carp (Aristichthys nobilis) myosin: The significance of ionic linkage effects and hydrogen bond effects. *Food Hydrocolloids, 102*, Article 105596. https://doi.org/10.1016/j.foodhyd.2019.105596

Sun, X., Yu, Y., Saleh, A., Akhtar, K., Li, W., Zhang, D., & Wang, Z. (2024). Conformational changes induced by selected flavor compounds from spices regulate the binding ability of myofibrillar proteins to aldehyde compounds. *Food Chemistry, 451*, Article 139455. https://doi.org/10.1016/j.foodchem.2024.139455

Wang, Y., Zhao, Y., He, Y., Ao, C., Jiang, Y., Tian, Y., & Lu, H. (2024). Effect of three unsaturated fatty acids on the protein oxidation and structure of myofibrillar proteins from rainbow trout (Oncorhynchus mykiss). *Food Chemistry, 451*, Article 139403. https://doi.org/10.1016/j.foodchem.2024.139403

Wu, Z., Shang, X., Hou, Q., Xu, J., Kang, Z., & Ma, H. (2024). Using ultrasonic-assisted sodium bicarbonate treatment to improve the gel and rheological properties of reduced-salt pork myofibrillar protein. *Meat Science, 212*, Article 109465. https://doi.org/10.1016/j.meatsci.2024.109465

Xu, P., Zheng, Y., Zhu, X., Li, S., & Zhou, C. (2018). L-lysine and L-arginine inhibit the oxidation of lipids and proteins of emulsion sausage by chelating iron ion and scavenging radical. *Animal Bioscience, 31*(6), 905–913. https://doi.org/10.5713/ajas.17.0617

Yu, Q., Hong, H., Liu, Y., Monto, A. R., Gao, R., & Bao, Y. (2024). Oxidation affects pH buffering capacity of myofibrillar proteins via modification of histidine residue and structure of myofibrillar proteins. *International Journal of Biological Macromolecules, 260*, Article 129532. https://doi.org/10.1016/j.ijbiomac.2024.129532

Zhang, D., Li, H., Emara, A. M., Hu, Y., Wang, Z., Wang, M., & He, Z. (2020). Effect of in vitro oxidation on the water retention mechanism of myofibrillar proteins gel from pork muscles. *Food Chemistry, 315*, Article 126226. https://doi.org/10.1016/j.foodchem.2020.126226

Zhang, D., Wu, Z., Ruan, J., Wang, Y., Li, X., Xu, M., & Li, H. (2022). Effects of lysine and arginine addition combined with high-pressure microfluidization treatment on the structure, solubility, and stability of pork myofibrillar proteins. *LWT, 172*, Article 114190. https://doi.org/10.1016/j.lwt.2022.114190

Zhang, H., Tian, X., Zhang, K., Du, Y., Guo, C., Liu, X., & Wang, W. (2022). Influence of content and degree of substitution of carboxymethylated cellulose nanofibrils on the gelation properties of cull cow meat myofibrillar proteins. *LWT, 153*, Article 112459. https://doi.org/10.1016/j.lwt.2021.112459

Zhang, T., Li, Z., Wang, Y., Xue, Y., & Xue, C. (2016). Effects of konjac glucomannan on heat-induced changes of physicochemical and structural properties of surimi gels. *Food Research International, 83*, 152–161. https://doi.org/10.1016/j.foodres.2016.03.007

Zhao, S., Yang, L., Hei, M., Zhao, Y., Zhu, M., Wang, H., & Ma, H. (2024). Conformation and functional modification of porcine myofibrillar protein by pepper leaf polyphenols under oxidative condition. *LWT, 198*, Article 116017. https://doi.org/10.1016/j.lwt.2024.116017

Zheng, J., Han, Y., Ge, G., Zhao, M., & Sun, W. (2019). Partial substitution of NaCl with chloride salt mixtures: Impact on oxidative characteristics of meat myofibrillar protein and their rheological properties. *Food Hydrocolloids, 96*, 36–42. https://doi.org/10.1016/j.foodhyd.2019.05.003

Zheng, Y., Xu, P., Li, S., Zhu, X., Chen, C., & Zhou, C. (2017). Effects of L-lysine/L-arginine on the physicochemical properties and quality of sodium-reduced and phosphate-free pork sausage. *International Journal of Nutrition and Food Sciences, 6*(1), 12–18. https://doi.org/10.11648/j.ijnfs.20170601.13

Zhou, A., Chen, H., Zou, Y., Liu, X., & Benjakul, S. (2022). Insight into the mechanism of optimal low-level pressure coupled with heat treatment to improve the gel properties of Nemipterus virgatus surimi combined with water migration. *Food Research International, 157*, Article 111230. https://doi.org/10.1016/j.foodres.2022.111230